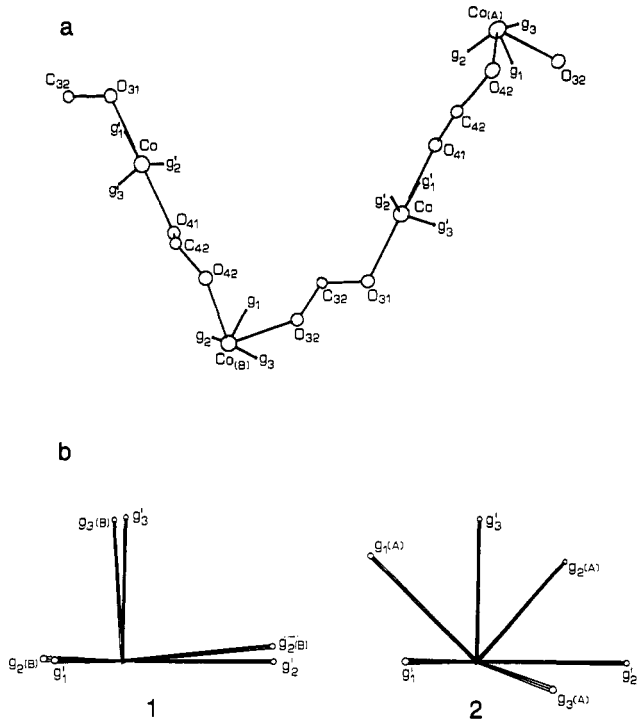

Figure 7. (a) Relative orientation of the g tensors of the cobalt(II) ions along the zigzag chain. (b) Comparison between the g tensor of the chelated cobalt(II) with those associated to the two hydrated neighbors: (a) Co_A and (2) Co_B (see Figure 4).

erence for the moments to align along the z axis (i.e. along the g'_3 direction). As far as the tensors of two consecutive hydrated cobalt ions (namely Co_A and Co_B in Figure 7a) have different orientations with respect to the tensor of the chelated cobalt, the two effective couplings along this direction (namely $J_\parallel$ and $J'_\parallel$) are expected to be different. In this respect, we observe that the g tensor of Co_A is, within experimental error, parallel to the g tensor of the chelated site, while the g tensor of Co_B is fully misaligned, with g_{3B} almost orthogonal to g'_{3B} (see Figure 7b). A simple estimate of the ratio $J'_\parallel/J_\parallel$ may be obtained examining the relative orientation of the moments associated to Co_A and Co_B, which are along the g_3 directions, with respect to g'_3. We obtain

$$\frac{J'_\parallel}{J_\parallel} = \frac{\cos\theta_B}{\cos\theta_A} \tag{7}$$

where θ_A (θ_B) refers to the angle between g'_3 and g_{3A} (g_{3B}). From Table I we calculate $\theta_A = 5°$ and $\theta_B = 82°$, and finally $J'_\parallel/J_\parallel \approx 0.1$. Notice that the structural factor pointed out above may reinforce this alternation since the largest exchange pathway ($J_\parallel$) involves at the same time the anti–anti configuration (see Figure 7a).

The strong dimerization observed in [CoCu] is more difficult to understand from the above arguments since copper(II) shows a small spin anisotropy. Anyway, an orbital reason may be still invoked in that case owing to the large orbital anisotropy of both ions. A detailed orbital study including the bridging carboxylate configurations should be now required in order to conclude this point.

Acknowledgment. This work was supported by the Comisiôn Interministerial de Ciencia y Tecnologia (Grant MAT89-177), and by the Italo-Spanish Integrated Action Number 41 and 27A. J.J.B.-A. thanks the Ministero de Educaciôn y Ciencia for a fellowship. The financial support of the Italian Ministry of Public Education and the CNR are gratefully acknowledged.

Registry No. $Co_2(EDTA)\cdot 6H_2O$, 84222-22-0; $CoCu(EDTA)\cdot 6H_2O$, 84222-24-2.

Contribution from the Institute for Chemical Reaction Science, Tohoku University, Katahira, Sendai, Japan 980

Temperature- and Axial-Ligand-Dependent EPR Spectra of Cobalt Porphyrin Cation Radicals: Effects of Mixing of the A_{1u} and A_{2u} States and a Locally Excited Triplet State

Minoru Satoh, Yasunori Ohba, Seigo Yamauchi, and Masamoto Iwaizumi*

Received October 10, 1990

The ground electronic states of cobalt tetraphenylporphyrin and octaethylporphyrin cation radicals ($Co^{III}TPP^{\bullet+}$, $Co^{III}OEP^{\bullet+}$) were reexamined by EPR spectroscopy. They are not purely an A_{1u} or A_{2u} state (nomenclature in D_{4h} symmetry), but they contain A_{1u} and A_{2u} components, respectively. The contribution of the A_{2u} state increases with increasing axial-ligand field. Equilibria were found between species having different axial-ligand interactions in solution. At low temperatures, the species having weaker axial-ligand interactions and having less A_{2u} character are dominant. The marked line width broadening observed for the EPR spectra of $Co^{III}OEP^{\bullet+}$ complexes ligated by Br^-, Cl^-, and CN^- was explained by the effect of mixing of a locally excited triplet state. Such mixing is less important for $Co^{III}TPP^{\bullet+}$ complexes having an A_{2u} dominant ground state.

Introduction

There have been extensive studies on the oxidation states of metalloporphyrins from biological and biochemical standpoints, as well as a physicochemical one in porphyrin chemistry. The oxidation of metalloporphyrins occurs at either the central metal or the porphyrin ring, or at the both locations. It is well-known that there are two types of ground states, A_{1u} and A_{2u}, in porphyrin cations. The cation radicals of cobalt tetraphenylporphyrin ($(Co^{III}TPP^{\bullet+})(X^-)_2$, X^- = axial ligands) have been assigned the A_{2u} ground state,[1] and no contradictory assignment has been reported. However, for the electronic state of the cobalt octaethylporphyrin cation radicals ($(Co^{III}OEP^{\bullet+})(X^-)_2$) assignments different from those originally given have been reported.

According to the UV–visible spectral criterion, $(Co^{III}OEP^{\bullet+})(ClO_4^-)_2$ was initially assigned the A_{2u} state, while when the counteranion ClO_4^- in $(Co^{III}OEP^{\bullet+})(ClO_4^-)_2$ was re-

*To whom correspondence should be addressed.

(1) (a) Ohya-Nishiguchi, H.; Khono, M.; Yamamoto, K. *Bull. Chem. Soc. Jpn.* **1981**, *54*, 1923. (b) Ichimori, K.; Ohya-Nishiguchi, H.; Hirota, N.; Yamamoto, K. *Bull. Chem. Soc. Jpn.* **1985**, *58*, 623. (c) Kadish, K. M.; Lin, X. Q.; Han, B. C. *Inorg. Chem.* **1987**, *26*, 4161.

0020-1669/92/1331-0298$03.00/0

placed by Br^-, the ground electronic state was considered to change from A_{2u} to A_{1u}.[2] Resonance Raman,[3] infrared,[4] and MCD[5] studies reported the same assignment as that from UV–visible spectroscopic studies on $(Co^{III}OEP^{\bullet+})(ClO_4^-)_2$ and $(Co^{III}OEP^{\bullet+})(Br^-)_2$. However, a recent resonance Raman study by Oertling et al.[6] and an ENDOR study by Sandusky et al.[7] assigned both $(Co^{III}OEP^{\bullet+})(ClO_4^-)_2$ and $(Co^{III}OEP^{+})(Br^-)_2$ complexes to the A_{1u} state. In the ENDOR study of Sandusky et al., the ground electronic state was also considered to be not the purely the A_{1u} state but a mixture with the A_{2u} state. Mixing of the A_{1u} and A_{2u} states in the ground electronic state has also been proposed in recent resonance Raman studies.[8] Prior to these ENDOR and resonance Raman studies, Morishima et al.[9] explained their temperature- and axial-ligand-dependent NMR data for $Co^{III}OEP^{\bullet+}$ by a model of thermal equilibrium between the A_{1u} and A_{2u} states.

It is known[10] that the a_{1u} and a_{2u} orbitals of the porphyrin ring have quite different spin distributions. Accordingly, EPR spectroscopy must be one of the most useful methods to elucidate the electronic state of porphyrin cation radicals. Though there have been a few EPR[1] and ENDOR[7] studies, it seems worthwhile to reexamine systematically the electronic state of cobalt porphyrin cation radicals by EPR spectroscopy. In this paper, we discuss the ground electronic state of the $Co^{III}OEP^{\bullet+}$ and $Co^{III}TPP^{\bullet+}$ complexes, focusing especially on the A_{1u} and A_{2u} mixing in the ground electronic state, on the basis of the temperature and axial-ligand dependence of the EPR spectra.

Experimental Section

$Co^{II}OEP$ and $Co^{II}TPP$ were prepared by using a previously published method.[11] Deuterium substitution at the meso positions of $Co^{II}OEP$ was accomplished by treating H_2OEP with D_2SO_4/D_2O,[12] and the substitution was confirmed by NMR spectroscopy. Tetrabutylammonium perchlorate (TBAP) was recrystallized from ethanol and dried in vacuo at 70 °C. Dichloromethane (CH_2Cl_2) was distilled over CaH_2 and stored over 4A molecular sieves in an ampule on a vacuum line. Commercially obtained GR grade $AgClO_4$, $AgPF_6$, and bromine were used without further purification. Chlorine prepared from H_2SO_4, NaCl, and MnO_2 was passed through a $KMnO_4$ solution and dried with $CaCl_2$. The 18-crown-6 complexes of potassium and sodium salts (18C6–KX, 18C6–NaX; $X^- = CN^-$, CH_3O^-, CH_3COO^-) were prepared by the method of Pedersen.[13]

$Co^{II}OEP$ and $Co^{II}TPP$ were oxidized by an electrochemical method or by bromine or chlorine in CH_2Cl_2. Electrochemical oxidation was performed by using TBAP as a supporting electrolyte or in the presence of 18C6–KX or 18C6–NaX together with the supporting electrolyte TBAP. $(Co^{III}OEP^{\bullet+})(PF_6^-)_2$ was prepared by adding $AgPF_6$ after bromine oxidation.

UV–visible and EPR spectra were recorded on Shimazu UV-240 and Varian E112 spectrometers, respectively. Magnetic field and microwave frequency were measured by an Echo Electronic NMR field meter, Type EFM-2000, and a Takeda Riken frequency counter, Type TR-5501, respectively. Temperatures were controlled by a nitrogen gas flow cryostat during the measurement of UV–visible and EPR spectra.[14] As the complexes of $Co^{III}OEP^{\bullet+}$ ligated by CN^-, CH_3O^-, and CH_3COO^- were unstable at room temperature, their spectral measurements were carried out at temperatures below −30 °C.

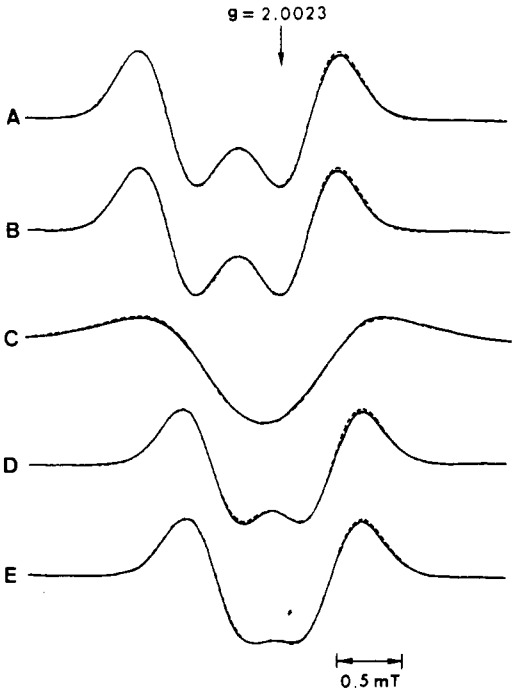

Figure 1. Second-derivative EPR spectra (—) and their simulations (---) for $(Co^{III}OEP^{\bullet+})(X^-)_2$ with various anions in CH_2Cl_2 at −70 °C: (A) $X^- = ClO_4^-$; (B) $Co^{III}OEP^{\bullet+}$-d_4 and $X^- = ClO_4^-$; (C) $X^- = Cl^-$; (D) $X^- = CH_3COO^-$; (E) $X^- = CH_3O^-$.

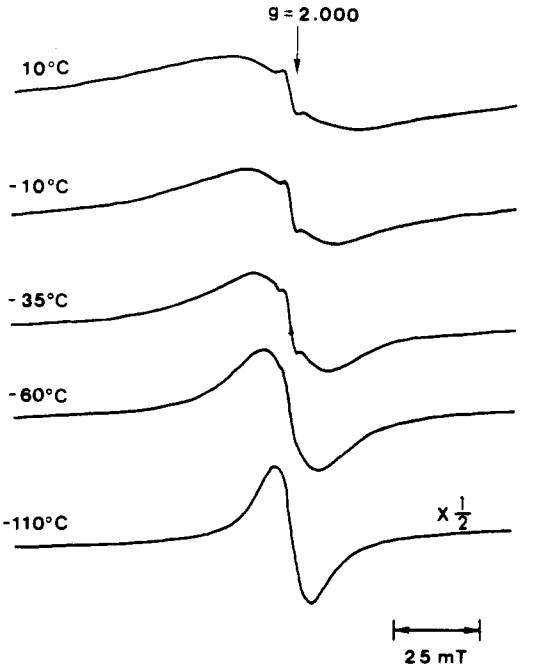

Figure 2. Temperature dependence of EPR spectra for $(Co^{III}OEP^{\bullet+})(Br^-)_2$ in CH_2Cl_2.

Results

UV–Visible Absorption Spectra. All the UV–visible absorption spectra observed for the $Co^{III}TPP^{\bullet+}$ system were of the so-called

(2) (a) Dolphin, D.; Addison, A. W.; Cairns, M.; Dinello, R. K.; Farrell, N. P.; James, B. R.; Paulson, D. R.; Welborn, C. *Int. J. Quantum Chem.* **1979**, *16*, 311. (b) Dolphin, D.; Muljiani, Z.; Rousseau, K.; Borg, D. C.; Fajer, J.; Felton, R. H. *Ann. N.Y. Acad. Sci.* **1973**, *206*, 177. (c) Dolphin, D.; Felton, R. H. *Acc. Chem. Res.* **1974**, *7*, 26. (d) Dolphin, D.; Forman, A.; Borg, D. C.; Fajer, J.; Felton, R. H. *Proc. Natl. Acad. Sci. U.S.A.* **1971**, *68*, 614.
(3) Kim, D.; Miller, L. A.; Rakhit, G.; Spiro, T. G. *J. Phys. Chem.* **1986**, *90*, 3320.
(4) Itoh, K.; Nakahashi, K.; Toeda, H. *J. Phys. Chem.* **1988**, *92*, 1464.
(5) (a) Browett, W. R.; Stillman, M. J. *Inorg. Chim. Acta* **1981**, *49*, 69. (b) Gasyna, Z.; Browett, W. R.; Stillman, M. J. *Inorg. Chem.* **1988**, *27*, 4619. (c) Gasyna, Z.; Stillman, M. J. *Inorg. Chem.* **1990**, *29*, 5101.
(6) Oertling, W. A.; Salehi, A.; Chang, C. K.; Babcock, G. T. *J. Phys. Chem.* **1989**, *93*, 1311.
(7) Sandusky, P. O.; Salehi, A.; Chang, C. K.; Babcock, G. T. *J. Am. Chem. Soc.* **1989**, *111*, 6437.
(8) Czernuszewicz, R. S.; Macor, K. A.; Li, X.-Y.; Kincaid, J. R.; Spiro, T. G. *J. Am. Chem. Soc.* **1989**, *111*, 3860.
(9) Morishima, I.; Takamuki, Y.; Shiro, Y. *J. Am. Chem. Soc.* **1984**, *106*, 7666.
(10) Gouterman, M. In *The porphyrins*; Dolphin, D., Ed.; Academic Press: New York, 1978; Vol. IV, p 1.
(11) Adler, A. D.; Longo, F. R.; Kampas, F.; Kim, J. *J. Inorg. Nucl. Chem.* **1970**, *32*, 2443.
(12) Bonnett, R.; Gale, I. A. D.; Stephenson, G. F. *J. Chem. Soc. C* **1967**, 1168.
(13) Pederson, C. J. *J. Am. Chem. Soc.* **1967**, *89*, 7017.
(14) Yamada, H.; Kikuchi, T.; Satoh, M.; Onodera, S.; Tokairin, S.; Iwaizumi, M. *Bull. Chem. Res. Inst. Non-Aqueous Solutions, Tohoku Univ.* **1988**, *38*, 1.

Table I. EPR Parameters for $(Co^{III}OEP^{\bullet+})(X^-)_2$ and $(Co^{III}TPP^{\bullet+})(X^-)_2$

complex	t/°C	g	ΔH_{pp}[a]/mT	hfcc/mT $\lvert a_{Co}\rvert$	hfcc/mT $\lvert a_N\rvert$	hfcc/mT $\lvert a_X\rvert$
$(Co^{III}OEP^{\bullet+})(ClO_4^-)_2$	20	2.0044	1.12	0.138	<0.01	
	−80	2.0044	1.10	0.138	<0.01	
$(Co^{III}OEP^{\bullet+})(CH_3COO^-)_2$	−70	2.0027	0.96	0.118	<0.01	
	−120[b]	2.0026	1.03	0.128	<0.01	
$(Co^{III}OEP^{\bullet+})(CH_3O^-)_2$	−70	2.0025	0.92	0.112	<0.01	
	−105[b]	2.0025	0.98	0.122	<0.01	
$(Co^{III}OEP^{\bullet+})(Cl^-)_2$	−10	2.0030	1.85			
	−90	2.0028	1.13	0.12		~0.05
$(Co^{III}OEP^{\bullet+})(Br^-)_2$	−10		26			
	−110[b]	2.000	11.4			
$(Co^{III}OEP^{\bullet+})(CN^-)_2$	−50	2.0034	4.8			
	−120[b]	2.0021	3.5			
$(Co^{III}TPP^{\bullet+})(ClO_4^-)_2$	20	2.0023	3.96	0.50	~0.16	
	−120[b]	2.0018	3.56	0.45	~0.16	
$(Co^{III}TPP^{\bullet+})(Br^-)_2$	25	2.011	10.0	1.24	~0.26	1.44
	−120[b]	2.008	9.0	1.15	~0.20	
$(Co^{III}TPP^{\bullet+})(Cl^-)_2$	20	2.0029	8.32	1.04	~0.28	~0.22
	−120[b]	2.0012	7.19	0.90	~0.20	

[a] The peak-to-peak line width in the first-derivative EPR spectra for the OEP complexes and the spread between the outermost peaks in the first-derivative EPR spectra for the TPP complexes. [b] Supercooling conditions.

A_{2u} type,[2] but for the series of $Co^{III}OEP^{\bullet+}$ complexes, two types of UV–visible spectra, so-called A_{1u} and A_{2u} types, were observed; $Co^{III}OEP^{\bullet+}$ ligated by ClO_4^-, PF_6^-, CH_3COO^-, and CH_3O^- showed the so-called A_{2u} type spectra, while $Co^{III}OEP^{\bullet+}$ ligated by CN^-, Br^-, and Cl^- showed A_{1u} type spectra.

EPR Spectra of $Co^{III}OEP^{\bullet+}$ Complexes. As Figure 1 shows, the EPR spectra of the $Co^{III}OEP^{\bullet+}$ complexes did not show drastic changes due to the axial ligand except for the complexes ligated by Br^-, Cl^-, and CN^-. In the complex ligated by Br^-, the EPR spectra showed marked line width changes with changes in temperature; at high temperatures the spectrum showed very broad line widths, and upon lowering of the temperature, the line widths decreased, accompanied by slight changes in the g value, as shown in Figure 2. At high temperatures, a sharp signal overlapping with the broad one was observed, but its signal intensity was about $^1/_{100}$th or less compared with that of the broad one; hence, it is not due to the main oxidation product. Spectral broadening at high temperatures was also observed for the complexes ligated by Cl^- and CN^-, though the broadening was not so remarkable as for the Br^- complex. In contrast to the case of these complexes, spectral changes with temperature were small in the complexes ligated by CH_3O^-, CH_3COO^-, and ClO_4^-. It is notable that in the latter complexes the spectral width rather increased upon lowering of the temperature. As will be stated later, this is due to an increase in the cobalt hyperfine coupling constant (hfcc), $|a_{Co}|$.

Hyperfine interactions were not resolved in the EPR spectra observed for the $Co^{III}OEP^{\bullet+}$ complexes. They were estimated by computer simulation of the spectra except for the case of the complexes ligated by Br^- and CN^-, whose spectral analysis was not made because determination of the hf couplings was difficult because of the large line width broadening effect. Spectral analysis for the complex ligated by Cl^- was made for the spectrum observed at −70 °C, because the line width broadening became negligible at low temperatures. The obtained EPR parameters are listed in Table I.

The values of $|a_{Co}|$ and $|a_N|$ and their axial-ligand dependence for the $Co^{III}OEP^{\bullet+}$ complexes studied here are much smaller than those for the $Co^{III}TPP^{\bullet+}$ complexes.[1] It can be seen from Table I that $|a_{Co}|$ decreases with increase of the axial-ligand field, because the ligand fields are considered to increase in the order CH_3O^- > CH_3COO^- > Cl^- > ClO_4^-. These changes in $|a_{Co}|$ are in strong contrast to those observed for the $Co^{III}TPP^{\bullet+}$ complexes, where they increase with increase of the axial-ligand field. It may be noted that the changes in g value are well correlated with those of $|a_{Co}|$, as shown in Figure 3. This correlation indicates that the g value is related to the spin–orbit coupling effect on the cobalt ion. Table I also shows that $|a_{Co}|$ slightly increases with lowering of the temperature.

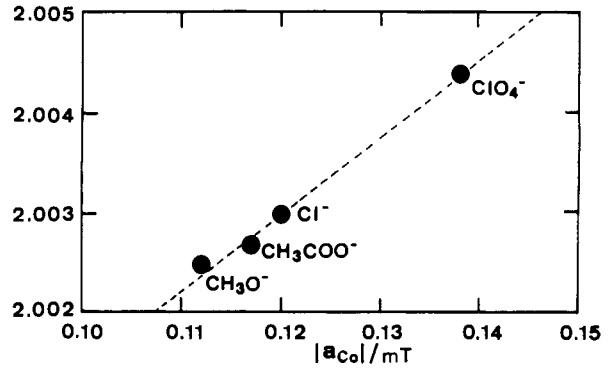

Figure 3. Correlation between $|a_{Co}|$ and the g value for $(Co^{III}OEP^{\bullet+})(X^-)_2$ (X^- = ClO_4^-, Cl^-, CH_3COO^-, CH_3O^-). The measurement temperature is −70 °C.

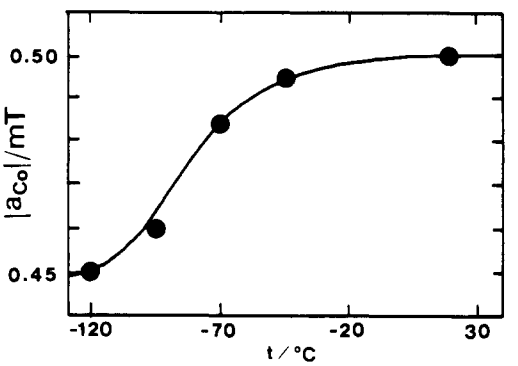

Figure 4. Temperature dependence of $|a_{Co}|$ for $(Co^{III}TPP^{\bullet+})(ClO_4^-)_2$.

The effect on the EPR spectra of deuterium substitution at the meso position was examined for the ClO_4^-, CH_3COO^-, and Cl^- complexes, and no appreciable effect was observed (Figure 1), indicating that the hfcc's of the meso protons do not contribute to the EPR line widths.

EPR Spectra of $Co^{III}TPP^{\bullet+}$ Complexes. The effects of axial ligands on the EPR spectra of $Co^{III}TPP^{\bullet+}$ complexes have been reported;[1a,b] it was shown that $|a_{Co}|$ and $|a_N|$ change markedly with axial ligands, and the stronger donative axial ligands produce larger $|a_{Co}|$ and $|a_N|$ values. In the present work, therefore, we examined mainly the temperature dependence of the EPR spectra in a few axial-ligand systems.

Figure 4 is a plot of $|a_{Co}|$ vs temperature for the $(Co^{III}TPP^{\bullet+})(ClO_4^-)_2$ system. It shows that $|a_{Co}|$ decreases with decreasing temperature. This change with temperature can be

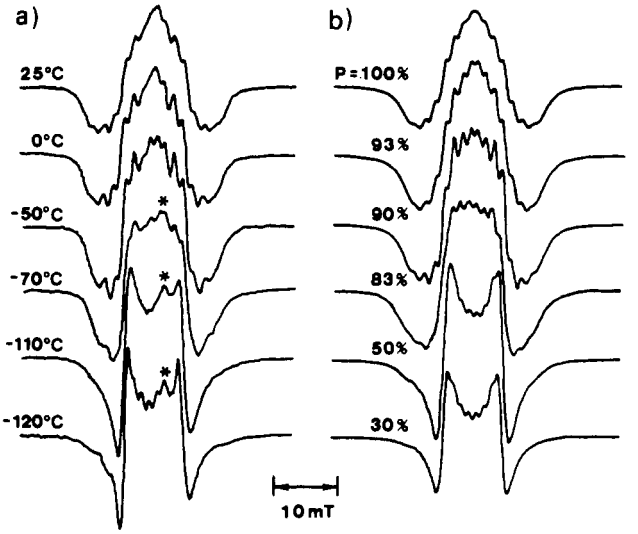

Figure 5. Temperature dependence of second-derivative EPR spectra for $(Co^{III}TPP^{\bullet+})(Br^-)_2$: (a) observed spectra; (b) calculated spectra. The percentages of the high-temperature species, P, are shown. The spectra were calculated by using the modified Bloch equation under the fast-exchange condition. The effect of intermolecular exchange of Br^- between the different complexes is not included. Asterisks indicate indefinable signals.

analyzed by assuming the presence of an equilibrium between two species having different hfcc's, a species having a larger hfcc and a species having a smaller one. The former species is dominant at low temperatures and the latter is dominant at high temperatures, and they are exchanging so rapidly compared to the EPR time scale that the observed hfcc's are statistically weighted averages of the hfcc's for the two species. The solid line in Figure 4 was calculated by using the hfcc's shown in Table I and the thermodynamic parameters, $\Delta H = -17$ kJ mol^{-1} and $\Delta S = 94$ J K^{-1} mol^{-1}, for the equilibrium A (low-temperature species) $\rightleftarrows$ B (high-temperature species).

Figure 5 shows the temperature dependence of the EPR spectra of $Co^{III}TPP^{\bullet+}$ ligated by Br^-. At high temperatures, the spectra show hf splittings due to two Br^- ligands, and as the temperature decreases, signals accompanied by no Br^- hf splittings appear. As Figure 5 shows, this spectral change can be well simulated by assuming that there is an equilibrium between the species showing Br^- hf splittings and the species showing no Br^- hf splittings and the equilibrium is in the fast-exchange limit on the EPR time scale. Such spectral changes indicate that the axial-ligand interaction becomes weaker with decreasing temperatures. It should be noted further that $|a_{Co}|$ is smaller for the species predominantly present at low temperature. The obtained hfcc's are listed in Table I, together with those for the $Co^{III}OEP^{\bullet+}$ complexes. One can see that the $|a_{Co}|$ values become larger at high temperatures for all the cases of $Co^{III}TPP^{\bullet+}$, in the reverse manner of those for the $Co^{III}OEP^{\bullet+}$ complexes.

Discussion

Electronic Ground State of $Co^{III}OEP^{\bullet+}$ Complexes Ligated by ClO_4^-, CH_3COO^-, and CH_3O^-. The $|a_{Co}|$ values observed for the $Co^{III}OEP^{\bullet+}$ system are much smaller than those for the $Co^{III}TPP^{\bullet+}$ complexes,[1] which have been identified as A_{2u} type radical complexes. They are also not sensitive to changes in the axial ligands. It is also notable that deuterium substitution at the meso positions does not affect the EPR spectral width; the hfcc at the meso protons may be less than 0.07 mT.[15] The meso proton hfcc of $(Mg^{II}OEP^{\bullet+})(ClO_4^-)$, which has been identified as an A_{1u} type radical complex, is 0.14 mT.[2c,16,17]

The above EPR spectral features are quite consistent with those expected from MO calculations; i.e., the a_{1u} unpaired electron orbital has nodes on the nitrogen and meso carbons and there is no overlap with the central metal orbitals, leading to the result that the hf couplings are less sensitive to the axial ligands. These features are the ones previously observed for the radical cations of Mg and Zn OEP complexes assigned as A_{1u} type radicals.[16,18]

These facts strongly suggest that the ground electronic states of $Co^{III}OEP^{\bullet+}$ complexes must be mainly of the A_{1u} type rather than A_{2u}, despite the fact that the complexes show the so-called A_{2u} type UV–visible absorption spectra, and there is no change in the ground electronic state from A_{1u} to A_{2u} due to the axial ligands. This assignment for the electronic ground state of the $Co^{III}OEP^{\bullet+}$ complexes is inconsistent with the assignment given in UV–visible,[2] infrared,[4] and MCD[5] studies and in the resonance Raman[3] study of Kim et al. However, it is consistent with the recent assignments in the resonance Raman studies of Oertling et al.[6] and Czernuszewicz et al.[8] and in Sandusky's ENDOR study.[7] This also indicates that the UV–visible spectral pattern does not necessarily provide correct information on the ground electronic state, though the use of such patterns has been one of the most convenient methods for the identification of the ground electronic states of the porphyrin radical cations. It should be noted however that the UV–visible spectral pattern is related not only to the ground state but also to the excited electronic states.

Changes in Spin Distribution Due to Axial Ligands and A_{1u}/A_{2u} State Mixing. As stated above, $|a_{Co}|$ values for the $Co^{III}TPP^{\bullet+}$ complexes generally increase with increasing axial-ligand fields,[1a,b] in the reverse manner for those of the $Co^{III}OEP^{\bullet+}$ complexes. For the $Co^{III}TPP^{\bullet+}$ complexes, a linear correlation between $|a_{Co}|$ and $|a_N|$ was found,[1a,b] and the correlation was explained by the formula

$$a_{Co} = Q_{N-Co}\rho_N + \alpha \qquad (1)$$

The first term in the right-hand side of eq 1 represents the contribution of the spin polarization through the Co–N bonds from the unpaired spin on the nitrogen atoms, and Q_{N-Co} and ρ_N are a proportionality constant with a negative sign for the spin polarization and the π spin density on the nitrogen atoms, respectively. The second term, α, is the contribution from the direct overlap between the unpaired spin orbital in the porphyrin ring and the cobalt orbitals, and it has a small positive value. For $Co^{III}TPP^{\bullet+}$, the first term provides the main contribution to $|a_{Co}|$, since ρ_N is large. Accordingly, in the $Co^{III}TPP^{\bullet+}$ complexes $|a_{Co}|$ increases with increasing ρ_N and a_{Co} is considered to have a negative sign. The fact that $|a_{Co}|$ increases with increasing axial-ligand field indicates that ρ_N increases with increasing axial-ligand field.

On the other hand, in the $Co^{III}OEP^{\bullet+}$ complexes $|a_{Co}|$ decreases with increase of the axial-ligand field. It is known that there is a node on the nitrogens in the a_{1u} orbital and hence there may be a negative spin density on them; therefore, the a_{Co} values for the $Co^{III}OEP^{\bullet+}$ complexes may be positive. The observed changes in $|a_{Co}|$ for the $Co^{III}OEP^{\bullet+}$ complexes may be well understood if it is assumed that the positive spin density is added to the negative spin density on the nitrogen atoms because of an increase in the axial-ligand fields, as in the case of the $Co^{III}TPP^{\bullet+}$ complexes. This leads to a decrease in $|a_{Co}|$ when the axial-ligand field increases, as experimentally observed.

It is notable here that the changes in $|a_{Co}|$ for $Co^{III}TPP^{\bullet+}$ due to axial ligands are very large; the observed maximum change amounts to 0.74 mT, which corresponds to nearly 60% of the

(15) The upper limit of the hfcc's was estimated by the computer simulation of the EPR spectra on the basis of the fact that there is no appreciable difference between the spectral patterns of the deuterated and undeuterated samples. The estimated value agrees well with the value for the $(Co^{III}OEP^{\bullet+})(ClO_4^-)_2$ complex, but it is smaller than that for the $(Co^{III}OEP^{\bullet+})(Cl^-)_2$ complex obtained by ENDOR.[7] The use of the hfcc obtained by ENDOR in the simulation calculations for $(Co^{III}OEP^{\bullet+})(Cl^-)_2$ did not give satisfactory results.

(16) (a) Fajer, J.; Borg, D. C.; Forman, A.; Dolphin, D.; Felton, R. *J. Am. Chem. Soc.* **1970**, *92*, 3451. (b) Hanson, L. K.; Chang, C. K.; Davis, M. S.; Fajer, J. *J. Am. Chem. Soc.* **1981**, *103*, 663.
(17) Fajer, J.; Borg, D. C.; Forman, A.; Felton, R. H.; Vegh, L.; Dolphin, D. *Ann. N.Y. Acad. Sci.* **1973**, *206*, 349.
(18) (a) Forman, A.; Borg, D. C.; Felton, R. H.; Fajer, J. *J. Am. Chem. Soc.* **1971**, *93*, 2790. (b) Fujita, I.; Hanson, L. K.; Walker, F. A.; Fajer, J. *J. Am. Chem. Soc.* **1983**, 105, 3296. (c) Ichimori, K.; Ohya-Nisiguchi, H.; Hirota, N. *Bull. Chem. Soc. Jpn.* **1988**, *61*, 2753.

maximum $|a_{Co}|$. According to the MO theory, the metalloporphyrin molecule has four a_{2u} orbitals. Mixing among these a_{2u} orbitals due to axial ligation will cause changes in the spin distribution. However, the LCAO atomic orbital coefficients of the nitrogen atoms in these a_{2u} orbitals are not different from each other by more than 30%,[19] and hence the observed large changes in $|a_{Co}|$ and $|a_N|$ for the $Co^{III}TPP^{\bullet+}$ complexes are apparently beyond the effect of mixing among the a_{2u} orbitals.

The observed changes in the spin distribution on the porphyrin ring due to the axial ligand are rather well explained in terms of A_{1u}/A_{2u} state mixing. The mixing occurs because of the pseudo-Jahn–Teller effect[8] and/or reduction of the molecular symmetry from D_{4h} to lower symmetry by the axial ligation. The ground electronic state of the $Co^{III}TPP^{\bullet+}$ complexes is considered to be A_{2u}-dominant, and but it also exhibits A_{1u} character. Since axial ligation elevates the a_{2u} orbital, the contribution from the A_{2u} state to the ground electronic state would increase by the increase in axial-ligand field; this leads to the increase of ρ_N and hence the increase of $|a_{Co}|$, as mentioned above.

On the other hand, for the $Co^{III}OEP^{\bullet+}$ complexes, the ground electronic state must be considered to be A_{1u}-dominant, but it exhibits a contribution from the A_{2u} state. When the axial-ligand field increases, the contribution from the A_{2u} state increases for the same reason as mentioned above. This leads to the addition of the positive spin densities on nitrogen atoms and hence a decrease in $|a_{Co}|$. This explains well the observed effects of axial ligands on $|a_{Co}|$.

Ichimori et al. have shown that the changes in hfcc's of the $Co^{III}TPP^{\bullet+}$ complexes due to axial ligands may be illustrated by MO calculations,[1b] but we should note that their calculations were done for molecules having S_4 symmetry. We confirmed by extended Hückel MO calculations that porphyrin molecules with planar structures cannot be affected to a large extent by axial ligation.

Temperature Dependence of Hfcc's and A_{1u}/A_{2u} State Mixing. It has been shown above that in the $Co^{III}TPP^{\bullet+}$ complex system there are equilibria between two species having different $|a_{Co}|$'s in solution and that the species having the smaller $|a_{Co}|$ is predominant at low temperatures. The fact that the Br^- hf splitting disappeared at low temperatures indicates that the species predominantly existing at low temperatures has weaker axial-ligand interaction, probably due to the increase in solvation of the respective cobalt porphyrin cation and anionic axial ligand. The spectra of the $Co^{III}OEP^{\bullet+}$ complex system could not be analyzed as those for the $Co^{III}TPP^{\bullet+}$ complexes because of the small temperature effect on the spectra, but it is likely that there are equilibria between the species having different interactions with axial ligands in the $Co^{III}OEP^{\bullet+}$ complexes, too.

As has been mentioned above, weakening the interaction with the anionic axial ligand leads to a reduction in the A_{2u} state contribution to the ground state. This indicates that the low-temperature species in the $Co^{III}TPP^{\bullet+}$ complexes have smaller $|a_{Co}|$'s and $|a_N|$'s, while those in the $Co^{III}OEP^{\bullet+}$ complexes have larger $|a_{Co}|$'s. This is in good agreement with the observed changes in the hfcc's due to temperature.

Morishima et al. have explained their temperature-dependent NMR data for some metalloporphyrin cation radicals by assuming thermal population between the A_{1u} and A_{2u} states.[9] According to their model, in the $Co^{III}TPP^{\bullet+}$ complexes the A_{1u} state is lying above the A_{2u} state and both states are thermally populated. If their model were valid, $|a_{Co}|$ would decrease at high temperatures. This contradicts the EPR data concerning the behavior of $|a_{Co}|$.

The present data clearly indicate that the A_{1u} and A_{2u} states are mixing in the ground state because of the pseudo-Jahn–Teller effect and/or reduction of molecular symmetry and that the mixing is affected by the axial-ligand interaction. It is also clear that there are equilibria between species having different axial-ligand interactions. The observed changes in $|a_{Co}|$ with temperature, therefore, can be attributed to the shift of the equilibria. The thermodynamic parameters for the equilibria have been determined from the spectral analysis of temperature-dependent EPR spectra of $Co^{III}TPP^{\bullet+}$ complexes. ΔH and ΔS were found to be in the ranges of −8 to −18 kJ mol^{-1} and 50 to 100 J K^{-1} mol^{-1}, respectively, but they could not be determined sufficiently accurately that changes in the parameters due to axial ligands can be discussed.

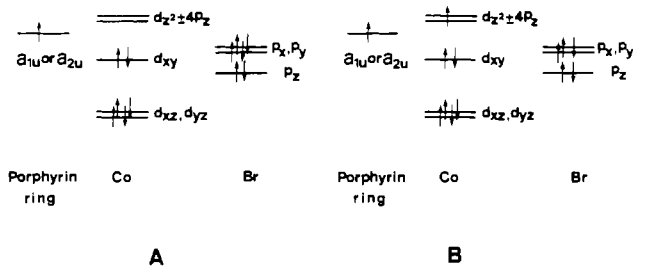

Figure 6. Electronic configurations in $(Co^{III}OEP^{\bullet+})(Br^-)_2$: (A) ground state; (B) excited state.

Spectral Broadening of $Co^{III}OEP^{\bullet+}$ Complexes Ligated by Br^-, CN^-, and Cl^-. As stated above, $Co^{III}OEP^{\bullet+}$ complexes ligated by Br^-, Cl^-, and CN^- show large line width broadening at high temperatures. The broadening of the Br^- complex is especially remarkable. Interestingly, line width broadening was not appreciable for the $Co^{III}TPP^{\bullet+}$ complexes. The spectral broadening observed for $Co^{III}OEP^{\bullet+}$ ligated by Br^-, CN^-, or Cl^- is beyond the effect of A_{1u}/A_{2u} mixing; the broadening is too large to be attributed to the contribution of the A_{2u} state or to the effects of hf couplings of the axial ligands. It is notable that the observed EPR spectral pattern has a Lorentzian line shape, indicating the presence of fast relaxation processes.

In view of the fact that the broadening was observed for the complexes ligated by Br^-, Cl^-, and CN^- having strong reducing power, it is most likely to attribute the line width broadening to the effect of mixing of a locally excited triplet state, which is shown in Figure 6.

The ground electronic state A in Figure 6 can mix with the excited electronic configuration B, through spin–orbit coupling, as expressed by

$$\Psi = \Psi_A - \frac{\lambda\langle\Psi_B|\hat{L}\hat{S}|\Psi_A\rangle}{E_B - E_A}\Psi_B \qquad (2)$$

where Ψ_A and Ψ_B are the wave functions for states A and B and E_A and E_B are their energies, respectively. As is seen from eq 2, the mixing of configuration B effectively occurs in the complexes with the anionic axial ligands having the HOMO at a high energy level. To the integral $\langle\Psi_B|\hat{L}\hat{S}|\Psi_A\rangle$ in eq 2, the two terms $\xi\langle\phi^{Co}(3d_{z^2} \pm 4p_z)|\phi^X(\pm p_z)\rangle\langle\phi^X(\pm p_z)|\hat{ls}|\phi^X(p_x, p_y)\rangle$ and $\xi'\langle\phi^{Co}(3d_{z^2} \pm 4p_z)|\hat{ls}|\phi^{Co}(3d_{yz}, 3d_{xz})\rangle\langle\phi^{Co}(3d_{yz}, 3d_{xz})|\phi^X(p_x, p_y)\rangle$ make the chief contribution, where $\phi^{Co}(3d_{z^2} \pm 4p_z)$ is the wave function for the cobalt orbitals used for the binding with the two axial ligands, $\phi^{Co}(3d_{yz}, 3d_{xz})$ is the wave functionfor the cobalt $3d_{yz}$ or $3d_{xz}$ orbital, and $\phi^X(\pm p_z)$ and $\phi^X(p_x, p_y)$ are the wave functions for the 2p orbitals of CN^-, 3p orbitals of Cl^-, or 4p orbitals of Br^-, respectively. The spin–orbit coupling, therefore, must be sensitively affected by the overlap between the cobalt and the axial-ligand orbitals. We have shown above that there are equilibria between species having different axial-ligand interactions. At high temperatures, the species having the stronger axial-ligand interaction would be predominant, and in such a species the mixing with the excited configuration B must be larger. The presence of such equilibria will cause the large line width broadening at high temperatures.

As mentioned above, the line width broadening was not remarkable in the $Co^{III}TPP^{\bullet+}$ complexes even when they were coordinated by Br^-. This may be attributed to the fact that in $CO^{III}TPP^{\bullet+}$ the a_{2u} orbital, which makes a large contribution to the unpaired electron orbital, has a direct overlap with $3d_{z^2} \pm 4p_z$, leading to an antiferromagnetic interaction between the unpaired spin on the a_{2u} orbital and cobalt $3d_{z^2} \pm 4p_z$ orbital. This will

(19) Longuet-Higgins, H. C.; Rector, C. W.; Platt, J. R. *J. Chem. Phys.* **1950**, *18*, 1174.

result in a decrease in the contribution from configuration B in the ground electronic state. The observed difference in the spectral broadening between the $Co^{III}TPP^{\bullet+}$ and $Co^{III}OEP^{\bullet+}$ complexes strongly suggests that the ground electronic states of the $Co^{III}OEP^{\bullet+}$ complexes are of the A_{1u}-dominant type even when they are coordinated by Br^-, Cl^-, or CN^-. Temperature-dependent NMR data for $(Co^{III}OEP^{\bullet+})(Br^-)_2$ have been explained by the effect of A_{1u}/A_{2u} thermal mixing, but this interpretation must be reexamined by taking into account the effect of configuration B on the NMR spectra.

Acknowledgment. This work was partially supported by Grant-in-Aid for Scientific Research No. 02453036 from the Ministry of Education, Science, and Culture of Japan.

Contribution from the Department of Chemistry, McGill University, 801 Sherbrooke Street West, Montreal, Quebec, Canada H3A 2K6

High-Pressure Infrared and Micro-Raman Spectra of Crystalline Pentacarbonyl(thiocarbonyl)chromium(0) and (η-Benzene)dicarbonyl(thiocarbonyl)chromium(0)

Yining Huang, Ian S. Butler,* and Denis F. R. Gilson*

Received May 29, 1991

Infrared spectra (4300-400 cm^{-1}) of crystalline $Cr(CO)_5(CS)$ and $(\eta\text{-}C_6H_6)Cr(CO)_2(CS)$ have been recorded at room temperature for pressures up to 25 and 30 kbar, respectively. High-pressure micro-Raman spectra of $Cr(CO)_5(CS)$ have been similarly investigated in the low-energy region (450-300 cm^{-1}) for pressures up to 25 kbar. The pressure dependences ($d\nu/dP$) of the IR-active, binary $\nu(CO)$ overtone and combination modes have been determined and used to calculate the pressure dependences of the parent $\nu(CO)$ fundamentals, which could not be determined directly, as these absorptions were hidden by the intense absorption of the diamond windows. There was no evidence of any pressure-induced phase transitions occurring in either complex over the pressure ranges investigated. The $d\nu/dP$ values for the CO and CS stretching modes suggest that in both complexes the π-back-bonding between the Cr and the CO groups is enhanced by increased pressure, while the Cr-CS π-back-bonding is increased for $Cr(CO)_5(CS)$, but the situation is not very clear for $(\eta\text{-}C_6H_6)Cr(CO)_2(CS)$. In addition, pressure selectively enhances the π-back-bonding to the CO group trans to CS in $Cr(CO)_5(CS)$.

The pressure dependences ($d\nu/dP$) of the $\nu(CO)$ modes in transition-metal carbonyl complexes provide useful information on the extent of π-back-bonding between the metals and the carbonyl groups.[1-7] Since the thiocarbonyl ligand (CS) is considered to be an appreciably better π-acceptor ligand than is CO,[8] we decided to extend our studies to two typical crystalline transition-metal thiocarbonyls, $Cr(CO)_5(CS)$ and $(\eta\text{-}C_6H_6)Cr(CO)_2(CS)$, and present here high-pressure IR data for these complexes, together with some high-pressure micro-Raman data for the low-frequency vibrations of the pentacarbonyl derivative.

Experimental Section

The thiocarbonyl complexes were prepared by the literature methods.[9-11] The experimental details for the high-pressure IR and micro-Raman work have been described elsewhere.[1] Raman spectra were recorded using 647.1-nm Kr ion laser excitation.

Results and Discussion

The pressure dependences and relative pressure dependences for the observed IR peaks of $Cr(CO)_5(CS)$ are given in Table I. The absence of any breaks in the slopes of the ν vs P plots up to 25 kbar indicates that there were no pressure-induced phase transitions throughout the pressure range investigated.

Table I. Vibrational Data for $Cr(CO)_5(CS)$

ν, cm^{-1}	$d\nu/dP$, cm^{-1}/kbar	d ln ν/dP, $kbar^{-1} \times 10^2$	assignt[a]
4172[b]	0.35	0.0084	$2\nu_1$, A_1
4118[b]	0.40	0.0097	$\nu_1 + \nu_{10}$, B_1
4092[b]	-0.006	-0.0001	$\nu_1 + \nu_2$, A_1
4048[b]	-0.35	-0.0085	$\nu_1 + \nu_{16}$, E
2088	0.18[c]	0.0086	ν_1, a_1, $\nu(CO^{eq})$
2017	0.22[c]	0.011	ν_{10}, b_1, $\nu(CO^{eq})$
2017	-0.18[c]	-0.0089	ν_2, a_1, $\nu(CO^{ax})$
1989	-0.53[c]	-0.027	ν_{16}, e, $\nu(CO^{eq})$
1289	-0.25	-0.019	ν_3, a_1, ν(CS)
1260	-0.09	-0.0072	
636	-0.46	-0.072	ν_4, a_1, ν_{17}, e, δ(CrCO)
	0.33	0.052	
512	0.16	0.030	ν_{18}, e, δ(CrCO)
487	0.21	0.043	ν_{19}, e, δ(CrCO)
427	0.73	0.17	ν_{20}, e, $\nu(Cr\text{-}CO^{eq})$
422	0.82	0.19	ν_5, a_1, $\nu(Cr\text{-}CO^{ax})$
381	0.78	0.20	ν_6, a_1, $\nu(Cr\text{-}CO^{eq})$
352	0.70	0.20	ν_7, a_1, ν(Cr-CS)

[a] From refs 12, 14, and 15. [b] Data obtained from $Cr(CO)_5(^{13}CS)$. [c] Data derived from overtone and combination bands.

Recent Raman studies have shown that the metal-CO interactions and the molecular geometries of metal carbonyl complexes are particularly sensitive to pressure.[1-7] Unfortunately, in contrast to our earlier work,[1-3] all attempts to record the micro-Raman spectra of $Cr(CO)_5(CS)$ under high pressure in both the $\nu(CO)$ and $\nu(CS)$ regions failed, because the peaks were inherently too weak to be monitored and extended data accumulation simply resulted in sample decomposition due to the necessary long exposures to the laser excitation. The corresponding IR peaks were quite intense, but an immense absorption due to the diamonds of the DAC completely masked the $\nu(CO)$ region. However, the $\nu(CS)$ region was free from interference. Also, we discovered that useful high-pressure data could be obtained from the binary $\nu(CO)$

(1) Huang, Y.; Butler, I. S.; Gilson, D. F. R.; Lafleur, D. *Inorg. Chem.* **1991**, *30*, 117.
(2) Huang, Y.; Butler, I. S.; Gilson, D. F. R. *Inorg. Chem.* **1991**, *30*, 1098.
(3) Huang, Y.; Butler, I. S.; Gilson, D. F. R. *Spectrochim. Acta* **1991**, *47A*, 909.
(4) Adams, D. M.; Ekejiuba, I. O. C. *J. Chem. Phys.* **1982**, *77*, 4793.
(5) Adams, D. M.; Davey, L. M.; Hatton, P. D.; Shaw, A. C. *J. Mol. Struct.* **1982**, *79*, 451.
(6) Adams, D. M.; Hatton, P. D.; Shaw, A. C.; Tan, T. K. *J. Chem. Soc., Chem. Commun.* **1981**, 226.
(7) Adams, D. M.; Ekejiuba, I. O. C. *J. Chem. Phys.* **1983**, *78*, 5408.
(8) Broadhurst, P. V. *Polyhedron* **1985**, *11*, 1801.
(9) English, A. M.; Plowman, K. R.; Butler, I. S.; Jaouen, G.; LeMaux, P.; Thepot, J.-Y. *J. Organomet. Chem.* **1977**, *132*, C1.
(10) English, A. M.; Plowman, K. R.; Butler, I. S. *J. Labelled Compd. Radiopharm.* **1980**, *17*, 641.
(11) Butler, I. S.; English, A. M.; Plowman, K. R. *Inorg. Synth.* **1982**, *21*, 1.

0020-1669/92/1331-0303$03.00/0